Bulletin of the Seismological Society of America. Vol. 48, pp. 315–337. October 1958

THE DESERT HOT SPRINGS EARTHQUAKES AND THEIR TECTONIC ENVIRONMENT

By C. F. Richter, C. R. Allen, and J. M. Nordquist

ABSTRACT

The Desert Hot Springs earthquake of December 4, 1948, was one of the larger recorded earthquakes of southern California, and its aftershocks have continued into 1957. The assigned epicenter is 33° 56.′4 N, 116° 23.′1 W; origin time, 15:43:16.7 P.S.T.; magnitude 6½. Arrival times at local and distant stations are consistent with existing travel-time curves, except for anomalous S − P intervals at very near-by temporary stations; these unexplained anomalies cannot be attributed to varying depth of focus.

Epicenters of the 72 aftershocks that have been accurately located are concentrated in a zone 18 km. long, parallel to the Mission Creek fault trace indicated by older scarps, but 5 km. north of it. Aftershock activity is markedly concentrated toward the two ends of this line. Location of the main shock suggests that fracturing started near the southeast end and progressed northwestward. The ground surface was not broken, except by landslides.

Offset of the line of seismic activity from the trace of the Mission Creek fault suggests that the fault plane dips north. This attitude is substantiated not only by field observations, but also by first motions at stations within 6° of the epicenter, which require a combination of thrust-slip and right lateral-slip on a fault dipping north less than 66°. Inasmuch as this fault is not parallel to regional San Andreas trend, such oblique displacement is reasonable and is consistent with the tectonic pattern of other faults in this region.

Five groups of earthquakes represent more than 85 per cent of the total strain release since 1933 in the 3,000 sq. km. area surrounding Desert Hot Springs. These earthquakes, in addition to the Desert Hot Springs shock, are: Morongo Valley (1947), Kitching Peak (1944), Covington Flat (1940), and San Gorgonio Mountain (1935); all are associated with known faults. The Morongo Valley earthquakes probably represent fracturing on the segment of the Mission Creek fault adjacent to that broken during the subsequent Desert Hot Springs shock.

Introduction

The Desert Hot Springs earthquake is of interest not only because of its relatively large magnitude of 6½, but also because it is one of the few large earthquakes for which detailed instrumental data are available on the aftershocks. This earthquake has been exceeded in magnitude by only three others in southern California within the past 50 years, and it would have caused considerable damage had it occurred in a metropolitan area rather than in a sparsely settled region of the southeastern California desert (fig. 1). Aftershocks are still continuing (1957), and their areal distribution forms one of the most interesting aspects of this study.

Portable instruments were operating in the epicentral area within 8 hours after the time of the main shock, and it is only the records of these very near-by stations that permit accurate locations of the aftershocks. Temporary stations that produced usable records were: Willis Palms (33° 49.′8 N, 116° 19.′9 W), Bennett Ranch (33° 55.′2 N, 116° 24.′4 W), and Desert Hot Springs (33° 57.′7 N, 116° 30.′0 W). The locations of these stations relative to the epicentral area are shown in figure 5. Other stations used in the routine locations were regularly established stations of the California Institute of Technology network, in addition to the Boulder City, Pierce Ferry, and Tucson stations of the U. S. Coast and Geodetic Survey.

Manuscript received for publication January 6, 1958.

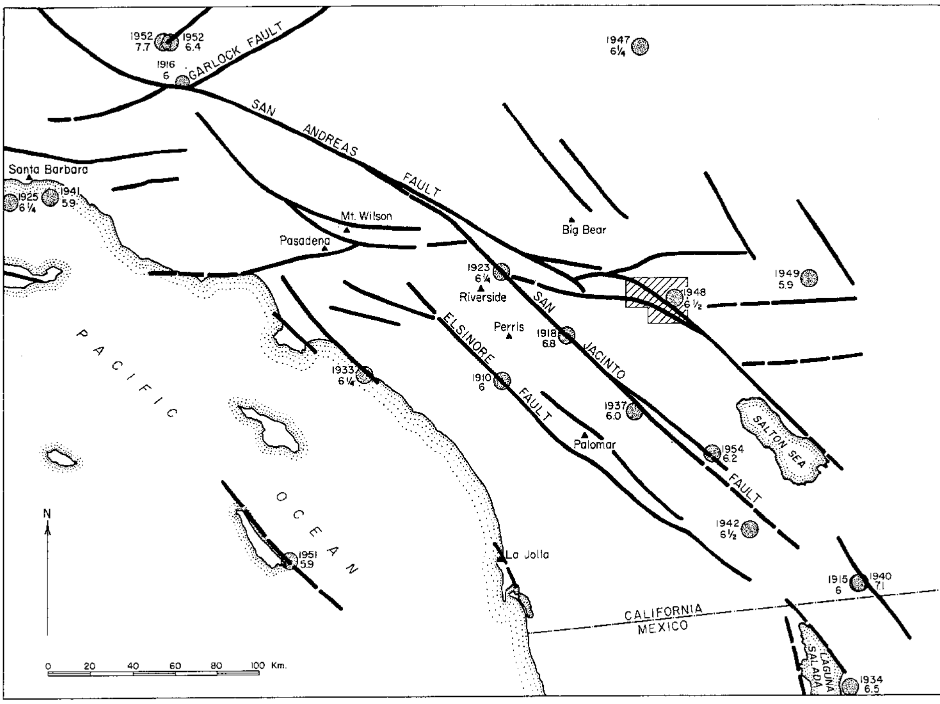

Fig. 1. Index map of southern California, showing major faults and epicenters of earthquakes of magnitude 5.9 or greater that have occurred within the past 50 years. The area of the Desert Hot Springs earthquakes (fig. 5) is shown by the diagonally hatched area.

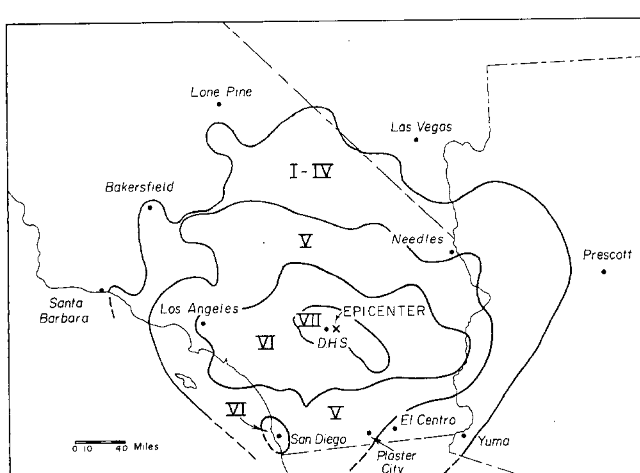

Fig. 2. Isoseismal map of the Desert Hot Springs earthquake of December 4, 1948, modified from U. S. Coast and Geodetic Survey (1949).

Macroseismic Effects

Field studies were carried out independently by the Seismological Field Survey of the U. S. Coast and Geodetic Survey and by the Seismological Laboratory, California Institute of Technology. Detailed notes for the latter group were prepared by Dr. M. E. Denson. Most of the field data collected by the two organizations were summarized in a mimeographed report of the U. S. Coast and Geodetic Sur-

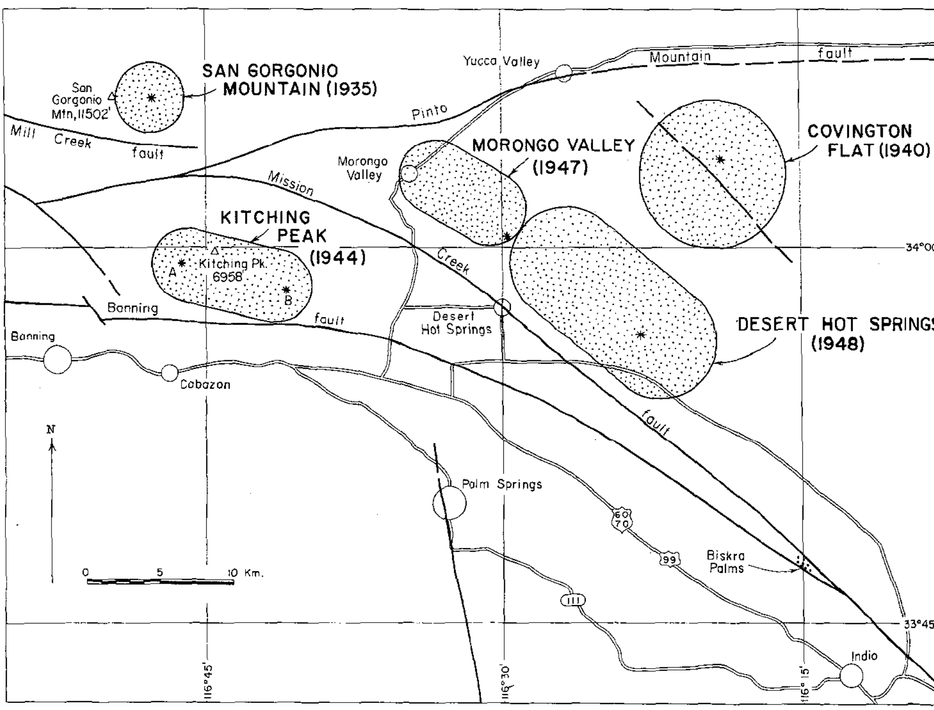

Fig. 3. Map of faults of the Desert Hot Springs region, showing epicentral areas of major earthquakes discussed in this study. Asterisks indicate locations of principal shocks. Stippled areas indicate roughly the areal spread of aftershocks.

vey (1949), and this report includes an isoseismal map from which figure 2 is redrafted with minor modifications. The field data were printed in a condensed but more widely circulated publication by Murphy and Ulrich (1951), although their map shows only the outer isoseismal.

The isoseismals are generally symmetrical, but a roughly east–west elongation is more pronounced for the higher intensities. This elongation parallels the trend of Transverse Range structures and is reflected in the extension of intensity VI into the alluvium of the Los Angeles basin. Minor damage was general in the metropolitan area, and inquiries reaching the Laboratory at Pasadena showed that claims were being adjusted for several years thereafter. Information from the Los Angeles City Board of Education supplied to the U. S. Coast and Geodetic Survey indicates that of 200 automatic gas shutoff valves belonging to the school system 14 were tripped; most of these were in the Monterey Park section, east of the city center.

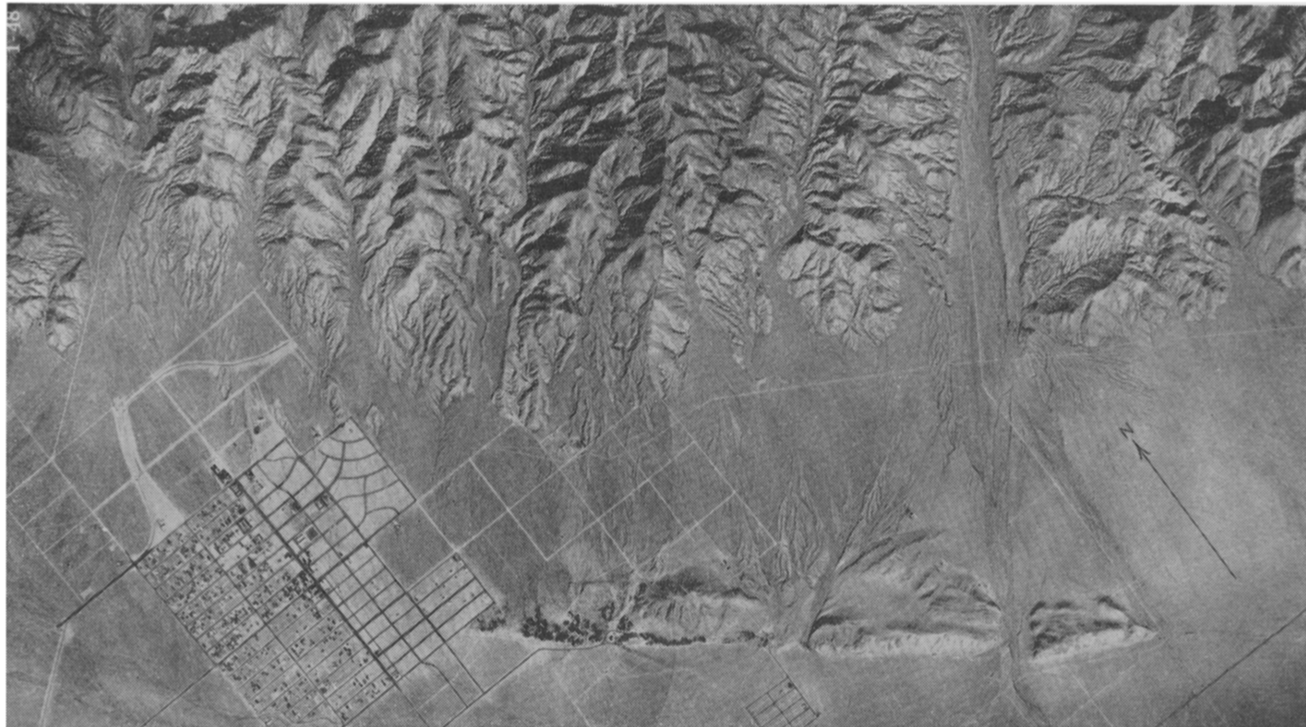

Fig. 4. Vertical aerial photograph of the Desert Hot Springs area, showing Recent scarps and springs along the trace of the Mission Creek fault (bottom). The town of Desert Hot Springs is at the left. Length of photograph is about 5 miles. Photographs by Fairchild Aerial Surveys, Inc.

Although San Diego and El Centro are at nearly the same epicentral distance (fig. 2), reported intensity was significantly higher at San Diego. This clashes with the natural expectation based on known "ground factor"; according to Gutenberg (1956, p. 759), the normal ground response at El Centro is roughly double that at San Diego. However, similar anomalies have been observed in other earthquakes where there is a marked difference in surface geology along different paths, and they have sometimes been described in terms of so-called "earthquake shadows." In the

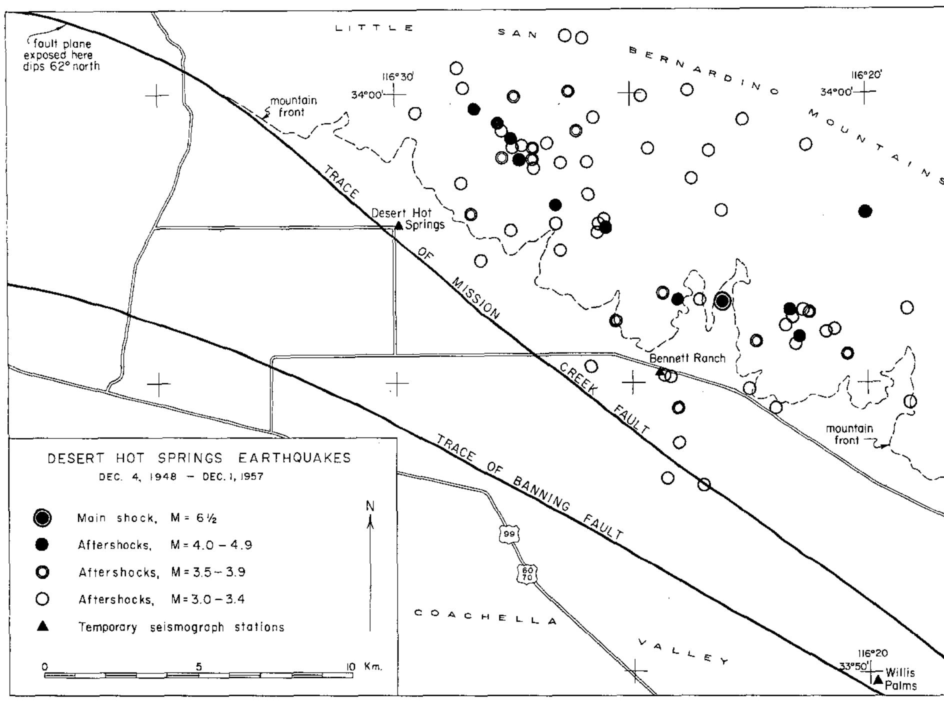

Fig. 5. Epicentral locations of the Desert Hot Springs earthquake and its aftershocks. Solid triangles represent locations of portable seismographs.

present instance, a possible explanation is that the disturbance traveled with relatively low attenuation through the rocks of the southern California batholith and emerged with locally increased amplitude into the alluvium and beach deposits around San Diego. But southeastward through the Imperial Valley, attenuation was high owing to the great thicknesses of lake beds, deltaic sediments, and Recent alluvium. This hypothesis is further supported by the reported intensity VI at Plaster City, which is on the west edge of the Imperial Valley at about the same distance as El Centro; the direct path was largely through the batholith, although the local ground is relatively unconsolidated.

The epicentral area within the Little San Bernardino Mountains was uninhabited, but dust clouds caused by massive landslides in this area were seen and photographed from as far away as Palm Springs. The surface of the ground was not broken, except by landslides and local fissures.

Geologic Setting

The Desert Hot Springs earthquake probably was caused by displacement on the Mission Creek fault, which is one of the major branches of the San Andreas fault system in southern California. Southeast of Cajon Pass, the San Andreas splits into several great branches, the most important of which appear to be the Banning fault, the Mission Creek fault, and the San Jacinto fault (figs. 1, 3). The Mission Creek

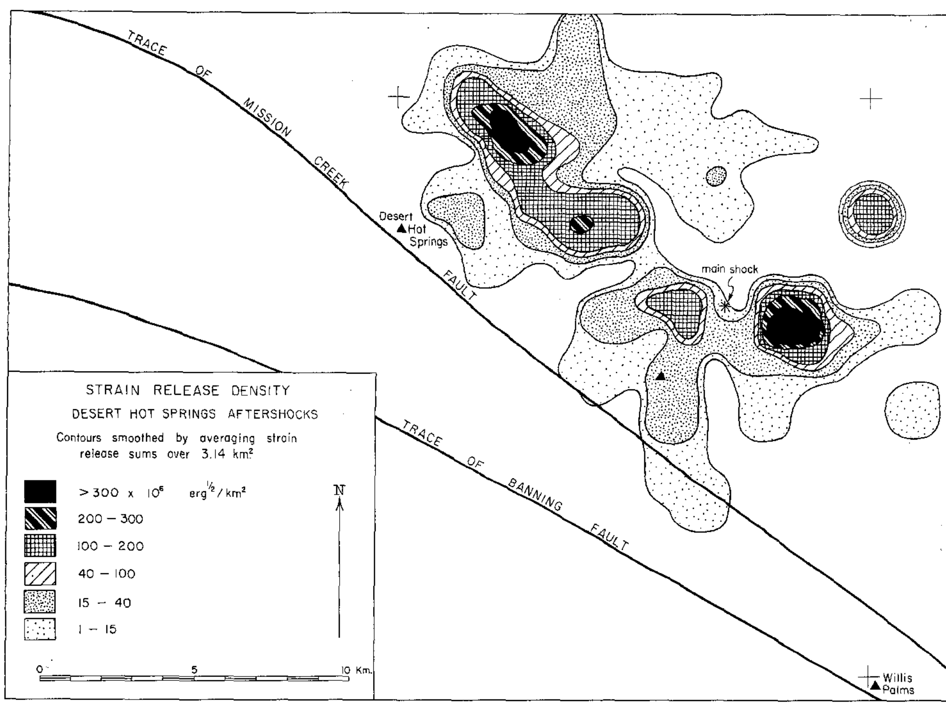

Fig. 6. Strain-release density map of the Desert Hot Springs aftershocks. See text for interpretation of this map.

fault diverges from the San Andreas fault at a high angle north of San Gorgonio Pass, and the geologic relations suggest that this area has been severely deformed in Quaternary time (Allen, 1957); possibly the Mission Creek fault was formerly aligned with the San Andreas fault so as better to absorb the lateral strain.

Within the San Bernardino Mountains, the Mission Creek fault dips 45° north and has not displaced Quaternary gravels. But farther east, where the fault curves gradually southward, Recent activity is indicated by prominent scarps and springs, such as are exemplified at Desert Hot Springs itself (fig. 4). The easternmost exposure of the fault plane, 4 km. west of the Twentynine Palms highway (fig. 5), reveals a northerly dip of 62°, and the linear trace of the fault to the southeast suggests that the fault plane gradually steepens in that direction. At Biskra Palms, 30 km. southeast of Desert Hot Springs, the Mission Creek fault joins the Banning fault at a low angle (fig. 3). The coalesced fracture beyond Biskra Palms has sometimes been called the San Andreas fault, but that this particular break deserves the parent name is debatable.

The Little San Bernardino Mountains, in which the epicentral area lies (fig. 5), are underlain primarily by amphibolitic gneisses whose migmatitic structures and variable composition reflect a complex geologic history. The age of these rocks is unknown. South of the mountains, only Tertiary and Quaternary sedimentary rocks are exposed in this area. Quaternary fanglomerates underlie most of the Indio Hills and comprise the Recent fault scarps at Desert Hot Springs. Alluvium and wind-blown sand cover the valley floor.

Near Desert Hot Springs the trace of the Mission Creek fault does not lie directly at the foot of the mountains, but instead cuts obliquely across the valley and through the Indio Hills. It is possible that an older, more easterly trending fault delimits the base of the range, but there is no physiographic or structural evidence for this other than the mountain front itself. The strain-release pattern of the Desert Hot Springs earthquakes (fig. 6) trends more nearly parallel to the Mission Creek fault than to a hypothetical break along the base of the Little San Bernardino Mountains.

Epicentral Locations

The individual Desert Hot Springs earthquakes have been located by using the previously established southern California travel-time curves (Gutenberg, 1951; Richter, 1955*a*). No reasons were found to modify these curves on the basis of this study, except perhaps at very short distances. Not all of the aftershocks were located independently; epicenters for most were determined by the method of time differences (Gutenberg, 1943, pp. 502–506) with respect to two well-located "key shocks," nos. 22 and 27 (table 2). These two shocks were chosen on the basis of (1) their locations toward the two ends of the line of epicenters, (2) the large number of stations for which records were available, including the near-by temporary station at Willis Palms, and (3) the internal consistency of data that permitted particularly good locations for these shocks. The following equations were used in the solutions:

$$P_n - O = K + \Delta/8.2 \qquad K = 5.4$$
$$p - O = D/6.34$$
$$D^2 = \Delta^2 + h^2$$

The first of the key shocks, no. 22, appeared on the basis of time differences to have almost identically the same epicenter as the much later shock no. 80, so the two solutions were combined to take advantage of the greater number of stations thus available. Arrival times for these and other critical shocks are given in table 1. The chosen epicenter (table 2) fits all the local stations for both shocks to within 2 km., and the chosen origin time agrees exactly with the Willis Palms S − P interval and is within 0.3 second of the origin times indicated by S − P intervals at Palomar, Riverside, Perris, and Crestline. Thus the epicentral location for shock no. 22 probably is good to within 2 km., granting the accuracy of the travel-time curves, and the depth of focus works out well at 16 km. If this epicenter is now used to establish revised values of K for the more distant stations, we find:

Station	K	Station	K
Pasadena	5.6	Tinemaha	7.0
Mount Wilson	5.5	Boulder City	6.0
La Jolla	5.2	Pierce Ferry	6.5
Haiwee	5.5	Tucson	5.4

The unusually high value of K for Tinemaha at this azimuth was also noted by Richter (1951) for the Manix earthquakes and can perhaps be attributed to the Sierran "root." Likewise noteworthy are the high values at Boulder City and Pierce Ferry.

Shock no. 27, at the opposite end of the line of epicenters from no. 22, was used as the second key shock. Its location probably is good to within 3 km., although the Willis Palms data demand a depth of about 10 km., and the internal consistency of the data is not as good as that of shock no. 22.

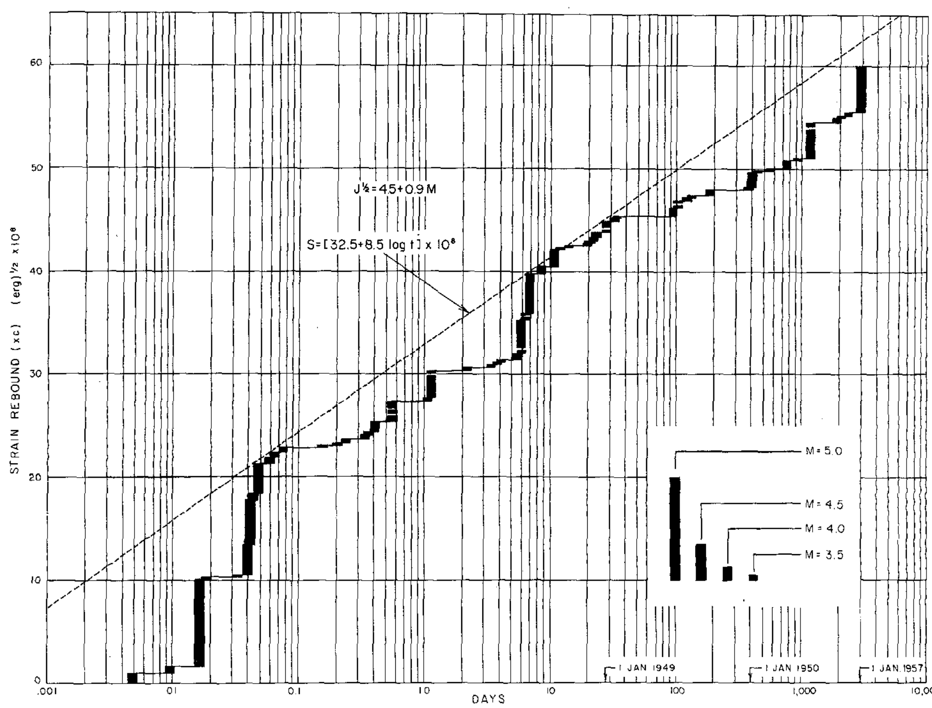

Fig. 7. Elastic-strain rebound characteristics of the Desert Hot Springs aftershocks.

Every aftershock with sufficient data was located by time differences with respect to each key shock independently, and the final epicenter (fig. 5) was chosen midway between the two points thus established—points which averaged 2.3 km. apart. Despite the large number of station records available, epicentral determinations by time differences were hindered by the fact that Riverside, Pasadena, and Mount Wilson lie at nearly the same azimuth from the epicentral area, as do Palomar and La Jolla. Indeed, accurate locations were virtually impossible without either (1) the Willis Palms data, or (2) a clear S $-$ P interval at Riverside. It is difficult to assign a measure of accuracy to the resulting locations, but it is felt that most are located to within 4 km. With this in mind, it is to be noted that figure 5 perhaps gives an undue impression of accuracy; however, the conclusions concerning the general zoning of the shocks and their concentrations toward the two ends of this zone are felt to be valid.

In deciding whether a particular earthquake should be considered an aftershock of the Desert Hot Springs group, only those have been included the epicenters of which fell within the general area outlined by shocks that occurred within the first few days following the main shock. A somewhat questionable case is the earthquake of January 31, 1957, which occurred more than 9 years later. Despite the fact that this is the only aftershock exceeding magnitude 4.0 that is well off the line of principal activity (fig. 5), it is included among the aftershocks because of its general proximity to the other shocks and because it fits well on the strain-release curve (fig. 7); indeed, it might almost have been expected on this basis alone.

The epicenter of the main shock is one of the poorer locations, owing to the lack of S − P intervals, the absence of very near-by stations at this time, and a seemingly anomalous arrival time at Palomar. Despite repeated attempts at reconciliation, the Palomar arrival is clearly one second late; no instrumental or other explanation seems satisfactory except for the existence of a local structural anomaly in this azimuth. Indeed, intermittently throughout the aftershock sequence, Palomar (and to some extent La Jolla) exhibit anomalous delays. A similar delay was noted in the Kitching Peak earthquakes of 1944, which occurred 15 miles west of Desert Hot Springs and are discussed later in this report.

The temporary stations established at Willis Palms, Bennett Ranch, and Desert Hot Springs were virtually within the epicentral area, and their records are of special interest. Many of these records show apparently anomalous arrival times and S − P intervals, although the shocks are not located with sufficient accuracy, nor are their depths of focus sufficiently well known, to allow a detailed study of these anomalies. In general, origin times computed from S − P intervals at these very near-by stations are earlier than those indicated by corresponding S − P intervals at Riverside, which is probably the most consistent of the permanent stations. For 13 shocks that were recorded at both Riverside and Willis Palms (most less than magnitude 3.0), origin times computed from the Willis Palms data average 0.9 second earlier than corresponding origin times based on the Riverside data. Likewise, Desert Hot Springs origin times average 0.5 second earlier than corresponding Riverside origin times for 15 shocks. Although the Bennett Ranch records also suggest early origin times, the spread in the data is too large for the average to be significant. Many of the shocks evidently originated at depths shallower than 16 km., but differences in origin times computed from S − P intervals cannot be attributed to this cause; apparently something more basic is involved.

Magnitudes

The magnitudes of aftershocks of the Desert Hot Springs group, and of other earthquakes included in the present study, are well established from the readings of amplitudes recorded by the standard torsion seismometers in southern California. For the principal Desert Hot Springs earthquake, however, all those seismometers recorded off scale.

Estimates of magnitude based on macroseismic effects are always rough. The radius of perceptibility of nearly 400 kilometers (250 miles) suggests magnitude approaching 7; but the lack of evidence for any intensity exceeding VIII would set a maximum magnitude near 6½. (See table 20 of Gutenberg and Richter, 1956.)

The strong-motion instruments at Pasadena recorded maximum trace amplitudes of 5.6 mm. (N–S) and 6.8 mm. (E–W), with periods about 0.8 sec. Using table 10 of Gutenberg and Richter (1942) for distance 150 km. gives $M = 6.4$.

TABLE 1

ARRIVAL TIMES OF INITIAL P AND S PHASES FOR CRITICAL SHOCKS

(Initial S phases are shown in parentheses. Station abbreviations are: BC—Boulder City, Cr—Crestline, H—Haiwee, LJ—La Jolla, MW—Mount Wilson, P—Pasadena, Pe—Perris, PF—Pierce Ferry, Pr—Palomar, R—Riverside, T—Tinemaha, TU—Tucson, WP—Willis Palms.)

	BC	H	LJ	MW	P	Pr	R	T	Tu	Others	
Desert Hot Springs										PF	
No. 1 (12–4–48) 15:43:	55.7	57.5	40.3	42.4	43.1 (65.0)	30.8	32.3	71.4	89.4	62.9	
										PF	WP
No. 22 (12–5–48) 01:28:	67.4	68.1 (106.3)	51.7 (68.0)	52.7 (70.7)	54.0 (70.6)	41.9	42.4 (52.3)	82.5 (140.4)		75.1	33.0 (36.0)
										WP	
No. 27 (12–5–48) 05:28:		92.9 (126.4)	74.5 (91.6)	77.2 (95.8)	78.2 (96.2)	64.7 (73.8)	66.7 (76.3)	106.6		54.5	
										Cr	Pe
No. 80 (6–7–50) 17:05:			45.4 (61.5)	46.4 (64.3)	47.6 (66.4)	35.4 (44.9)	36.2 (46.2)			35.3 (45.2)	34.6 (43.6)
Morongo Valley											
No. 1 (7–24–47) 14:11:	35.6	26.1 (63.2)	10.2 (26.2)	10.5 (30.3)	11.9 (32.4)	00.8	00.4 (10.6)	39.8 (93.8)	61.2		
Covington Flat											
No. 1 (5–17–40) 21:04:	38.2	39.7	25.7 (45.0)	26.1 (45.4)	26.9 (47.1)	15.6	16.3 (27.8)	53.4	73.5		
Kitching Peak											
No. 1 (6–10–44) 03:12:	31.0	28.4 (63.2)	12.0 (27.2)	10.2 (24.0)	11.3 (26.6)	02.9 (10.5)	00.0 (06.7)	42.2 (95.3)	66.5		
No. 4 (6–12–44) 02:45:	75.0	73.0 (108.3)	56.2 (71.9)	55.5 (69.5)	56.4 (71.7)	46.8	44.8 (52.2)	87.1 (143.0)	110.0		
San Gorgonio Mtn.											
No. 1 (10–24–35) 06:48:		44.4	31.2	28.4	29.2 (44.7)		17.7 (25.0)	59.1			

Since Tinemaha is off scale, the trace amplitude exceeds 120 mm. Using this amplitude, distance 390 km., and station correction −0.2 gives $M = 6.3$ as a minimum.

For torsion seismometers at the northern California stations, readings of trace amplitudes were kindly supplied by Mr. John E. Meeker. The results are as follows:

Station	Δ km.	A_N mm.	A_E mm.	Correction	M
Mount Hamilton	600	50.2	35.5	+0.1	6.7
Palo Alto	640	62.0	49.0	−0.1	6.7
Mineral	840	31.8	20.6	?	6.8

Maximum amplitudes of surface waves with periods near 20 seconds reported in the bulletins of distant stations were as follows:

Station	Δ deg.	A_N μ	T sec.	A_E μ	T sec. sec.	Correction	M
Tacubaya	21	106	16	106	16	?	6.0
La Paz	68	3	20	3.5	20	+0.4	6.0
Cheb	85	..	..	10	20	0	6.3
Praha	86	7	19	6	20	0	6.1
Cartuja	86	80	20	...	..	0	7.1
Sverdlovsk	90	5	?	...	..	0	5.9
Riverview	110	1	18	1	19	+0.3	5.7

Body-wave amplitudes are reported only by Cartuja, which gives PZ 4μ, period 3 sec. and SE 29μ, period 18 sec. These give $m = 7.0$ (corresponding to $M = 7.1$). The value of M from Tacubaya cannot be given much weight because of the relatively short period of the maxima reported. The other Mexican stations report maxima wth still shorter periods. The Soviet bulletin does not give the component or the period for Sverdlovsk; here it assumed that 5 microns is the combined amplitude, and that the period is near 20 seconds.

The results at Cartuja look suspiciously high; a moderate error in determining or applying magnification would account for the discrepancy. The consistently low values of M at the other stations, compared with those from local stations, are in agreement with observation in other earthquakes of magnitude below 6.7. The general result cannot be considered precise, but 6.5 has been adopted, with an uncertainty of ± 0.2.

Times Recorded at Distant Stations

The magnitude of the main shock is hardly sufficient to warrant a full-scale study of recorded times; moreover, international seismology had not yet recovered from the effects of war.

Table 3 is a revision of the entry in the International Seismological Summary (volume for 1948, pp. 672–674), presenting readings reported in station bulletins.

Distances have been calculated from 33° 56′ N 116° 23′ W (direction cosines $A = -0.37020$, $B = -0.74446$, $C = +0.55563$); they differ by no more than 0°.2 from those tabulated in the Summary, calculated from 33°.9 N 116°.3 W.

The columns headed "P − O obs." and "S − O obs." give travel times from 23:43:17 G.C.T., 2 seconds less than those given in the Summary, which takes O = 23:43:15.

TABLE 2

DESERT HOT SPRINGS EARTHQUAKES OF MAGNITUDE 3.0 AND GREATER

(All times and dates are in Pacific Standard Time. "NL" in the location column indicates that the data were insufficient for an accurate location.)

Shock no.	Date	Origin time	Mag.	Location	
1	12- 4-48	15:43:16.7	6½	33-56.4	116-23.1
2	12- 4-48	15:46	3.9	NL	
3	12- 4-48	15:58	3.7	NL	
4	12- 4-48	16:03	3.4	NL	
5	12- 4-48	16:07:21.0	4.9	33-56.3	116-21.6
6	12- 4-48	16:10	3.1	NL	
7	12- 4-48	16:27	3.1	NL	
8	12- 4-48	16:40:32.4	4.4	33-55.8	116-21.4
9	12- 4-48	16:42:35.3	4.6	33-57.7	116-25.6
10	12- 4-48	16:46:20	3.6	NL	
11	12- 4-48	16:50:57.0	4.4	33-59.7	116-28.3
12	12- 4-48	17:06:26.0	3.6	33-56.1	116-25.3
13	12- 4-48	17:16:30.2	3.5	33-56.6	116-24.3
14	12- 4-48	17:33:41.8	3.4	33-55.8	116-20.8
15	12- 4-48	18:21:24.1	3.1	33-59.6	116-25.8
16	12- 4-48	19:27:02.3	3.0	33-58.0	116-23.0
17	12- 4-48	20:35:48.5	3.1	33-55.9	116-23.8
18	12- 4-48	21:20:50.8	3.4	33-54.7	116-19.1
19	12- 4-48	23:47:48.5	3.4	33-59.2	116-27.3
20	12- 5-48	00:26:21.9	3.0	NL	
21	12- 5-48	00:33:00.9	3.0	33-59.4	116-27.7
22	12- 5-48	01:28:28.9	3.9	33-59.1	116-27.4
23	12- 5-48	04:24:55.3	3.0	33-55.6	116-24.6
24	12- 5-48	04:51:26.8	3.7	33-57.9	116-28.4
25	12- 5-48	05:17:46.6	3.5	33-59.1	116-27.3
26	12- 5-48	05:20:45.4	3.2	33-58.5	116-28.6
27	12- 5-48	05:28:52.2	3.5	33-54.6	116-24.0
28	12- 5-48	14:25:55.3	3.1	34-00.1	116-23.7
29	12- 5-48	16:45:56.4	3.0	33-57.8	116-25.5
30	12- 5-48	18:46:07.7	4.3	33-59.5	116-27.8
31	12- 5-48	18:51:25.5	3.2	34-00.1	116-28.5
32	12- 6-48	07:58:58.8	3.0	33-53.2	116-24.3
33	12- 6-48	20:49:20.1	3.3	33-59.1	116-24.6
34	12- 7-48	12:05:44.5	3.0	33-56.1	116-21.5
35	12- 7-48	14:55:30.8	3.0	33-55.1	116-24.2
36	12- 8-48	00:37:54.5	3.0	33-54.8	116-22.5
37	12- 8-48	11:33:54.0	3.2	33-58.8	116-26.5
38	12- 8-48	17:26:59.5	3.2	33-56.3	116-19.1
39	12-10-48	01:18:02.7	3.1	33-57.7	116-27.5
40	12-10-48	02:58:54.8	3.5	33-55.7	116-22.3
41	12-10-48	08:53:07.3	3.0	33-53.9	116-24.0
42	12-10-48	12:09:14.9	3.1	33-58.3	116-25.8
43	12-10-48	12:42:57.0	4.4	33-56.4	116-24.0

TABLE 2—*Continued*

Shock no.	Date	Origin time	Mag.	Location	
44	12–10–48	21:18:55.4	3.1	33–57.8	116–25.7
45	12–10–48	23:13:33.8	3.1	33–57.3	116–26.4
46	12–10–48	23:22:04.8	3.1	33–58.8	116–27.0
47	12–11–48	08:12:19.5	4.5	33–58.1	116–26.6
48	12–11–48	10:15:28.7	3.3	33–59.2	116–26.7
49	12–13–48	00:19:13.7	3.1	33–57.8	116–26.5
50	12–13–48	02:14:05.0	3.1	33–58.8	116–25.9
51	12–13–48	07:01:14.9	3.2	33–59.7	116–29.6
52	12–13–48	07:09:34.7	3.0	33–37.2	116–28.1
53	12–15–48	08:41:48.6	3.8	33–56.2	116–21.2
54	12–16–48	14:57:21.8	3.2	33–55.1	116–24.4
55	12–18–48	13:07:59.3	3.1	33–55.3	116–25.8
56	12–22–48	06:30:48.6	3.0	33–59.2	116–21.2
57	12–23–48	14:59:51.6	3.2	33–55.6	116–21.5
58	12–24–48	15:27	3.2	NL	
59	12–26–48	01:25:21.1	3.3	NL	
60	12–27–48	15:36:02.6	3.5	33–59.4	116–26.1
61	12–31–48	21:24:26.9	3.0	33–56.3	116–21.3
62	1– 1–49	01:05:32.2	3.3	33–59.1	116–23.3
63	1– 1–49	07:11:28.0	3.6	33–59.8	116–27.5
64	1– 5–49	21:54:14.3	3.4	33–56.5	116–23.5
65	1– 7–49	00:23	3.0	NL	
66	2– 2–49	22:20:52.8	3.0	33–59.6	116–22.6
67	3– 5–49	01:36:37.5	3.2	33–53.3	116–23.5
68	3– 7–49	04:56:10.3	3.1	34–00.0	116–24.7
69	3– 8–49	10:22:26.3	3.4	33–56.0	116–21.6
70	3–15–49	07:08:51.4	3.4	34–01.1	116–26.3
71	3–15–49	11:42	3.0	NL	
72	4– 1–49	11:20:03.3	3.0	33–59.1	116–27.5
73	4– 3–49	15:34:27.5	3.4	34–01.0	116–25.8
74	4–17–49	10:09:17.6	3.1	33–55.9	116–20.7
75	6– 6–49	04:23	3.5	NL	
76	10–10–49	16:25	3.0	NL	
77	12–10–49	06:50	3.2	NL	
78	1–12–50	21:07:20.4	4.1	33–58.9	116–27.4
79	2– 9–50	19:31:52.0	3.6	34–00.1	116–26.3
80	6– 7–50	17:05:22.5	3.2	33–59.1	116–27.4
81	12–29–50	19:48:09.0	3.7	33–58.9	116–27.1
82	6– 7–51	01:52:53.5	3.0	33–54.6	116–21.9
83	7–17–51	06:50:32.8	3.2	34–00.5	116–28.7
84	1– 7–52	22:34:28.2	4.4	33–59.3	116–27.5
85	1–27–52	16:09:57.5	3.5	33–55.5	116–20.4
86	12– 9–53	03:53:55	3.3	NL	
87	12–20–53	15:15:50.8	3.1	33–58.6	116–23.7
88	7– 9–54	09:22:31	3.1	NL	
89	3–16–55	06:51:47	3.3	NL	
90	1–31–57	23:52:15.0	4.6	33–58	116–20

TABLE 3

TIMES FOR MAIN SHOCK

(Assumed origin time: 1948 December 4, 23:43:17 G.C.T. Distances Δ calculated from 33° 56′ N, 116° 23′ W. Direction cosines: $A = -0.37020$, $B = -0.74446$, $C = +0.55563$.

Station	Δ	P − O obs.	P − O 1955	O − C	S − O obs.	S − O calc.	O − C
Palomar	00.7	00:14	00:14	0			
Riverside	00.9	00:15	00:16	−1			
La Jolla	01.2	00:23	00:21	+2			
Mount Wilson	01.4	00:25	00:24	+1			
Pasadena	01.5	00:26	00:25	+1	00:50	00:46	+4
Boulder City	02.5	00:39	00:39	0	(01:11)	01:11	0
Haiwee	02.5	00:41	00:39	+2			
Santa Barbara	02.8	00:45	00:43	+2			
Tinemaha	03.5	00:54	00:53	+1			
Fresno	03.9	01:01	00:58	+3			
Tucson	04.9	01:12	01:11	+1	02:16	02:12	+4
Lick	05.5	01:21	01:20	+1	02:19	02:29	
Santa Clara	05.6	01:39	01:21		03:05	02:32	
Branner	05.8	01:26	01:24	+2	02:49	02:35	+14
Berkeley	06.2	01:31	01:30	+1	02:52	02:45	+7
San Francisco	06.2	01:33	01:31	+2	02:41	02:45	−4
Mineral	07.6	01:54	01:51	+3	03:58	03:18	
Shasta	08.3	02:03	02:02	+1	04:13	03:38	
Logan	08.6	02:06	02:06	0	04:24	03:43	
Ferndale	09.1				04:13	03:59	+14
Arcata	09.2	02:18	02:15	+3	04:17	04:00	+17
Bozeman	12.4	03:06	03:01	+5	05:34	05:18	+16
Butte	12.4	03:11	03:01	+10	05:40	05:18	+22
Rapid City	14.4	03:24	03:27	−3	06:26	06:06	+20
Victoria	15.5	03:47	03:40	+7	06:42	06:31	+11
Lincoln	17.2	04:04	04:01	+3	07:26	07:11	+15
Saskatoon	19.5	04:36	04:28	+8	08:14	08:01	+13
Tacubaya	21.1	04:54	04:45	+9	08:43	08:36	+8
St. Louis	21.6	04:51	04:51	0	09:02	08:46	+16
Chicago	24.0	05:15	05:16	−1	09:37	09:29	+8
Mobile	24.1	05:29	05:17	+12	09:48	09:31	
Sitka	26.9				10:31	10:17	+14
Cleveland	28.5	05:53	05:57	−4	10:48	10:44	+5
Columbia	29.3				10:56	10:56	0
New Kensington	29.8				11:15	11:03	+12
Ville Marie	30.8	06:16	06:18	−2			
State College	31.2	06:13	06:22	−9	11:37	11:26	+11
Rolphton	31.7	06:25	06:26	−1			
Ottawa	33.0	06:36	06:38	−2	11:58	11:54	+4
Philadelphia	33.3				12:14	11:59	+15
Fordham	34.2	06:48	06:48	0	12:24	12:13	+11
Shawinigan Falls	35.2	07:10	06:57	+13			
Harvard	35.9	07:03	07:02	+1	12:55	12:39	+16
Seven Falls	36.6	07:07	07:08	−1	12:57	12:50	+7
Halifax	41.6	07:53	07:49	+4	14:13	14:05	+8
San Juan	47.3	08:32	08:34	−2	15:35	15:29	+6
Bogotá	48.9	08:47	08:46	+1	16:02	15:51	+11

TABLE 3—*Continued*

Station	Δ	P − O obs.	P − O 1955	O − C	S − O obs.	S − O calc.	O − C
Huancayo	60.2	10:10	10:07	+3			
La Paz	68.1	11:03	11:00	+3	20:03	20:02	+1
Lisbon	81.2	12:18	12:17	+1			
Vladivostok	81.2	12:19	12:17	+2	22:26	22:25	+1
Paris	81.3	12:18	12:18	0			
Clermont-Ferrand	83.7	12:32	12:31	+1			
Strasbourg	84.0	12:33	12:32	+1			
Stuttgart	84.5	12:35	12:34	+1			
Basel	84.6	12:34	12:35	−1			
Cheb	84.9	12:31	12:37	−6	22:50	23:03	
Zurich	85.2	12:38	12:38	0	23:18	23:05	+13
Malaga	85.4	12:40	12:39	+1			
Cartuja	85.6	12:41	12:40	+1	23:28	23:10	+18
Praha	85.7	12:43	12:41	+2	23:31	23:12	+19
Alicante	86.7	12:14?			22:54		
Trieste	88.9				23:30	23:41	
Sverdlovsk	89.6	12:57	12:58	−1	23:53	23:48	+5
Tamanrasset	101.1	13:52	13:50	+2			
Stalinabad	107.8	14:30	14:21	+9			

Times in the column "P − O 1955" are those given by Gutenberg (1955), based on readings of the Kern County earthquake of July 21, 1952; residuals O − C in the next column follow by subtracting these from the observed times.

Times in the column headed "S − O calc." are based on the standard tables by Jeffreys and Bullen (1940), using the means between those tabulated for a surface source and for depth "0.00," which is believed to represent focal depth of about 33 kilometers. They have been further modified by applying corrections determined by Gutenberg (1955), as follows: from 20° to 40°, + 1 sec.; near 48°, + 2 sec.; at 68°, + 3 sec.; from 80° to 86°, + 1 sec.; near 89°, + 2 sec. Residuals in the following column headed "O − C" are based on these corrected times.

The fit is excellent in general. Late readings for P are prevalent only in the range from 12° to 21°, where the first motion is usually small. The S readings show the same effect, but are also sometimes late at greater distances, which is to be expected for a shock no larger than this.

There are no good observations of PKP, and apparently also none of SKS. Readings given for S at Alicante and Cheb are early, and might represent SKS; however, the times of P given for these stations are also too early.

For P the data were examined for mean residual and standard error. Seven Falls reported time was increased by one minute. The time reported for Huancayo as that of S was taken as representing P; this was confirmed by examining the original seismograms, now on file at Pasadena. Eight stations reporting P were omitted from the first reduction. Santa Clara, Butte, Mobile, and Shawinigan Falls obviously have recorded late phases. Cheb gives a time 6 seconds too early, but this is actually only reported to the nearest tenth of a minute. The time for Alicante is also too early, and is questioned in the original station bulletin. That at State College is impossibly early. Stalinabad time has been omitted, but only because of the general uncertainty of travel times in the shadow zone of P.

There remain 52 stations; the mean O − C residual is +1.21 sec., with standard error ±2.44 sec. To dispose of the effects of small amplitudes of P in the range between 9° and 22°, a separate reduction was carried out omitting the 8 stations at those distances. For these 44 stations the mean residual is +0.70 sec., with standard error ±1.61 sec. This shows that there are no systematic differences between the times of this shock and those of the 1952 shock studied by Gutenberg; all deviations are well within the limits of observational error.

Strain Characteristics

A graphic portrayal of the aftershock strain release is shown in figure 6, which was prepared by a method somewhat similar to that of St. Amand (1956). Each aftershock was assigned a strain-release figure based on the simplified magnitude equation,

$$\log J = 9.0 + 1.8\,M$$

Following Benioff (1951), it is assumed that for each shock the strain release is proportional to the square root of the energy. A strain-release "density" figure was thus assigned to each of 400 equally spaced points on the map by using an areal averaging technique similar to that used in the preparation of petrofabric diagrams (Fairbairn, 1949, chap. 21). Averages were computed for successive and overlapping circles of 1 km. radius; a greater or lesser degree of averaging, or "smoothing," could have been attained by varying the arbitrarily assigned size of this test area. The resulting strain-release density figures have been contoured and patterned in figure 6, again in a manner similar to that used in petrofabric diagrams.

In the interpretation of figure 6, note that (1) the main shock has not been included in the contouring, although its position has been marked; (2) the contour intervals do not represent equal increments of strain-release density; and (3) the unit $\text{erg}^{\frac{1}{2}}/\text{km.}^2$ is not dimensionally correct for areal strain density, because it includes the dimensional constant relating strain and energy. A quantitative measure of the true strain density would require knowledge of the volume of strained rock, the elastic constants, and the fraction of stored energy that had been converted into seismic waves (Benioff, 1951, p. 42).

Two aspects of the strain-release density map deserve special mention: the offset of the line of activity from the surficial trace of the Mission Creek fault, and the concentrations of strain release toward the two ends of the active zone.

The aftershock epicenters are concentrated in an elongate zone 18 km. in length, parallel to the trace of the Mission Creek fault but 5 km. north of it. Although this offset might be used as an argument against the association of this earthquake with the Mission Creek fault, a more reasonable hypothesis is that the fault plane dips north and thus effectively displaces the epicenters from the surface trace. Assuming a hypocentral depth of 16 km., the 5 km. offset indicates an average dip of 73° for the fault plane. This agrees well with the geologic observations: exposures of the fault plane 13 km. northwest of Desert Hot Springs (fig. 5) indicate a 62° northerly dip, and the regional geology suggests a steepening dip toward the southeast.

The concentrations of aftershock strain release toward the two ends of the epicentral zone are particularly interesting in view of the similar results from the Kern

County earthquakes (Benioff *et al.*, 1954; Benioff, 1955*a*). Inasmuch as the Kern County and Desert Hot Springs earthquakes are among the very few shocks exceeding magnitude 6 the aftershock distributions of which have been studied in detail, the generality of this apparent concentration is not known; possibly it is a widespread phenomenon in large earthquakes. Instead of being a manifestation of elastic afterworking or stress relaxation, Benioff (1955*b*) has suggested that it might be caused by "forward creep of the strain rock in response to an altered stress pattern resulting from the principal earthquake." Another possibility is that previous slippages on the fault have left "glued" and "unglued" segments that cause marked differences in strain-energy accumulation at various points along the fault, and that the aftershock concentrations do in reality represent areas of high strain-energy density prior to faulting.

It is interesting to note that the aftershock strain release is remarkably balanced between the two ends of the Desert Hot Springs zone of activity. If a line is drawn midway between the two principal concentrations (fig. 6), 51 per cent of the strain was released in the southeast segment and 49 per cent in the northwest segment.

The epicentral location of the main Desert Hot Springs shock suggests that fracturing commenced near the southeast end of the epicentral zone and progressed northwestward. This unidirectional progression of faulting, too, is similar to the pattern of the Kern County earthquakes and apparently represents a widespread phenomenon in large earthquakes (Richter, 1955*b*).

Figure 7 shows the cumulative strain-release curve for the Desert Hot Springs aftershocks through September, 1957. Following $t = 0.05$ day, the simplest envelope is given by the straight line: $S = (32.5 + 8.5 \log t) \times 10^8$. The general shape of this curve is similar to that of many aftershock sequences but differs markedly from others; this problem has been discussed in detail by Benioff (1951, 1955*a*). It has not been possible to plot the strain release from the two sides of the fault separately, as proved interesting for the Kern County aftershocks.

In order to compare strain characteristics of the Mission Creek fault in this earthquake with those of the White Wolf fault in the Kern County earthquakes, computations have been made assuming the same elastic constants and energy-magnitude relationship as used by Benioff (1955*b*). The volume of the strained rock is assumed to be 4.6×10^{18} cm.^{3}, using a 35 km. depth and an area outlined by the zone of aftershock activity. The average strain in this volume prior to the main shock was 2.7×10^{-5}; of this total, 2.1×10^{-5} was in elastic strain, and 0.6×10^{-5} was in creep strain, assuming that all the aftershocks represent creep strain recovery. The average elastic stress was 10 kg/cm.^{2}, and the elastic strain energy density was 108 erg/cm.^{3} These figures are of the same order of magnitude as those given by Benioff (1955*b*) for the White Wolf fault. By using the modified magnitude equation (Gutenberg and Richter, 1956) the average displacement along the Mission Creek fault is calculated very roughly as 30 cm.

First Motions and Tectonic Implications

The magnitude of the Desert Hot Springs earthquake was not sufficiently large to permit a fault-plane solution using world-wide stations. On the other hand, certain limits can be placed on the orientation of the fault displacement by applying techniques of the fault-plane solution to stations within about 6° of the epicenter.

The strike of the fault plane can be estimated to within 2° by the direction of its trace and by the orientation of the line of aftershock activity. This attitude, together with the reported compressions in the San Francisco area, demand that the dip of the fault plane be at least as shallow as 65°, which is consistent with the other field and seismic data. When the fault-plane circle is drawn using this dip, there is still considerable leeway in drawing the auxiliary circle, which defines the sense of movement within the fault plane. If the fault dips 65°, however, the compressions at Riverside and Tucson[1] require that the rake of the net slip be less than 74°, and the dilatation at Palomar requires that the rake be greater than 10°. Thus the first motions demand an oblique displacement, which must be a combination of thrust-slip and right lateral-slip. First motions at all the other near-by stations are consistent with this interpretation.

Oblique displacement on the Mission Creek fault is also supported by field evidence: The Little San Bernardino Mountains themselves suggest relative uplift of the north block, and Dibblee (1954, p. 26) presents evidence of right-hand strike-slip movement along this fault in the Indio Hills, southeast of Desert Hot Springs. From a tectonic point of view, oblique displacement on the Mission Creek fault is reasonable, if not to be expected. Stresses of the San Andreas type (i.e., maximum principal stress oriented slightly west of north) applied to a north-dipping fault of this trend should result in exactly the postulated oblique movement, inasmuch as the fault trace here is not parallel to the general San Andreas trend. This part of California is a region of conflict between San Andreas and Transverse Range structures, and it is to be expected that the present movements on faults do not necessarily reflect the strain patterns under which the breaks originally formed. In San Gorgonio Pass, west of Desert Hot Springs, abundant evidence testifies to the deformation and breaking-up of previous lines of faulting, including the Mission Creek fault itself (Allen, 1957).

Regional Seismic History and Associated Faults

The area of the Desert Hot Springs earthquakes was characterized by low seismic activity in the years prior to 1948 for which records are available. Indeed, no earthquakes exceeding magnitude 3.6 had occurred since 1934 in the area of subsequent Desert Hot Springs activity. On the other hand, the surrounding region has been the locus of a number of moderate earthquakes during this time interval, and the locations of the four largest of these are shown in figure 3, together with the Desert Hot Springs epicentral area. Strain-release sums for shocks of magnitude 3.0 and over for these five series of earthquakes are as follows:

Earthquake	Dates	Strain Release ($\times C$)
Desert Hot Springs	12- 4-48 to 2- 1-57	284×10^8 (ergs)$^{\frac{1}{2}}$
Morongo Valley	7-24-47 to 11-14-47	117×10^8 (ergs)$^{\frac{1}{2}}$
Covington Flat	5-17-40 to 1-21-42	107×10^8 (ergs)$^{\frac{1}{2}}$
Kitching Peak	6-10-44 to 11- 1-44	60×10^8 (ergs)$^{\frac{1}{2}}$
San Gorgonio Mtn	10-24-35 to 11-11-35	22×10^8 (ergs)$^{\frac{1}{2}}$

These five groups of earthquakes represent more than 85 per cent of the strain release in the area of figure 3 since January 1, 1934; most of the remaining activity

[1] Examination of the Tucson seismograms indicates that the International Seismological Summary for 1948 is mistaken in reporting a dilatation at Tucson.

has been in the form of small shocks in the northwestern part of this area. No great earthquakes are known from the historical records, although the abundance of Recent scarps along the Banning, Mission Creek, and Pinto Mountain faults testifies to major seismic events within Recent geologic time.

Morongo Valley earthquakes.—The Morongo Valley earthquakes, which occurred about a year prior to the Desert Hot Springs earthquake, are of particular interest because the Morongo Valley epicenters lie along the northwesterly extension of the Desert Hot Springs line of activity (fig. 3). Probably these two groups of earthquakes represent fracturing along adjacent segments of the Mission Creek fault, so that they must be closely related tectonic events. The Morongo Valley earthquakes commenced with two foreshocks, and the main shock ($M = 5.5$) was followed in the 10 succeeding days by 15 aftershocks of magnitude greater than 4.0 (table 4). The strain-release pattern is more similar to that of the Imperial Valley earthquake "swarms" than to the pattern of the subsequent Desert Hot Springs series. Arrival times for the main shock are given in table 1.

TABLE 4

MORONGO VALLEY EARTHQUAKES OF MAGNITUDE 4.0 AND GREATER

(Epicenter "A" indicates a location close to that of the main shock, placed at 34° 00'.5 N, 116° 29'.8 W. Epicenter "B" indicates a more northwesterly location, in the area of 34° 03' N 116° 33' W.)

Shock no.	Date	Origin time	Mag.	Epicenter
1	7-24-47	14:10:47.3	5.5	A
2	7-24-47	14:53:42	4.3	A
3	7-24-47	14:54:27	4.9	A
4	7-24-47	16:46:32	5.0	A
5	7-24-47	17:56:48	4.6	A
6	7-24-47	21:17:53	4.3	A
7	7-24-47	22:19:50	5.2	A
8	7-24-47	23:57:31	4.2	A
9	7-25-47	08:14:54	4.5	B
10	7-25-47	17:24:14	4.2	A
11	7-25-47	18:49:42	5.1	A
12	7-26-47	15:04:26	4.5	B
13	7-26-47	15:13:52	4.1	B
14	7-29-47	08:36:16	4.2	B
15	7-29-47	21:22:18	4.4	B
16	8- 1-47	09:01:38	4.1	B
17	8- 7-47	22:47:46	4.0	B

Data are insufficient to permit accurate location of all the Morongo Valley shocks, but comparisons of arrival times suggest that many of the epicenters lie as much as 8 km. northwest of the main shock, which is placed at 34° 00'.5 N, 116° 29'.8 W. This suggests that the pattern of fracturing was similar to that of the Desert Hot Springs earthquake; breaking probably commenced at the southeast end of the fractured zone and extended northwestward. None of the Morongo Valley shocks appears to have occurred within the area of subsequent Desert Hot Springs activity, and hence the Morongo Valley earthquakes can hardly be considered foreshocks of the Desert Hot Springs earthquake.

TABLE 5

KITCHING PEAK EARTHQUAKES OF MAGNITUDE 3.0 AND GREATER

(Epicenter "A" indicates a location close to that of shock no. 1, placed at 33° 59½′ N, 116° 46½′ W. Epicenter "B" indicates a location close to that of shock no. 4, placed at 33° 58½′ N, 116° 41′ W. The relative positions of these two epicenters are shown in figure 2.)

Shock no.	Date	Origin time	Mag.	Epicenter
1	6-10-44	03:11:50.8	4.5	A
2	6-10-44	03:15:32.2	4.0	A
3	6-10-44	03:26:12.4	3.2	A
4	6-12-44	02:45:35.0	5.1	B
5	6-12-44	02:49:56.2	3.7	B
6	6-12-44	03:13:46.1	3.5	B
7	6-12-44	03:16:36.2	5.3	B
8	6-12-44	03:39:09.9	3.6	B
9	6-12-44	03:48:47.4	3.4	B
10	6-12-44	05:45:27.9	3.8	B
11	6-12-44	06:43:20.7	3.5	B
12	6-12-44	12:22:58.6	3.6	B
13	6-12-44	14:21:19.5	4.2	B
14	6-12-44	16:19:28.6	3.7	B
15	6-13-44	05:20:49.7	3.2	B
16	6-13-44	09:30:14.5	3.7	B
17	6-13-44	10:37:05.9	3.3	B
18	6-13-44	16:04:36.2	3.9	B
19	6-13-44	17:20:44.6	3.3	B
20	6-13-44	19:31:49.6	3.3	B
21	6-14-44	01:46:32.5	3.5	B
22	6-15-44	12:44:23.3	3.8	B
23	6-17-44	15:41:03.3	3.4	B
24	6-20-44	05:42:23.2	3.2	B
25	6-23-44	13:28:42.8	3.6	B
26	6-27-44	08:34:50.2	3.4	A
27	6-27-44	22:55:17.4	3.5	A
28	6-28-44	02:19:51.4	3.3	B
29	6-29-44	19:04:44.5	3.3	B
30	7- 1-44	02:53:59.1	3.7	B
31	7- 7-44	04:39:29.7	3.0	B
32	8-22-44	01:48:54.3	3.0	B
33	8-22-44	10:22:30.8	3.1	B
34	8-24-44	23:30:25.5	4.2	B
35	8-24-44	23:37:34.9	3.0	B
36	8-24-44	23:38:12.2	3.1	B
37	8-28-44	04:53:14.5	3.1	A
38	8-29-44	14:46:47.8	3.0	A
39	9-20-44	06:12:22.6	3.6	B
40	10-28-44	10:30:17.8	4.4	A
41	11- 1-44	03:46:31.4	3.1	A
42	4- 6-45	07:46:46.0	3.6	A
43	9- 7-45	07:34:25.0	4.3	A
44	9- 7-45	07:45:30.2	3.0	A

Covington Flat earthquakes.—These earthquakes commenced less than 24 hours prior to the Imperial Valley earthquake of May 18, 1940, and systematic analysis of the aftershocks is difficult because seismic records of the two events are intermixed. Macroseismic effects have been described by Neumann (1942, p. 20).

The Covington Flat series started with a shock of magnitude 5.4, and this was followed by a normal aftershock sequence that lasted for somewhat over a year. Only the principal shock is permissive of accurate epicentral location; it is at 34° 03½′ N, 116° 19′ W, which is in Lower Covington Flat about 8 miles southeast of the town of Yucca Valley (U.S.G.S. Joshua Tree, California, quadrangle). The chosen epicenter is about 3 km. from the epicenter determined by Gutenberg (1943, p. 509) from earlier travel-time data, and is about 2 km. from the location inferred by residuals from the Desert Hot Springs key shock no. 22. Comparison of arrival times of the aftershocks with those of the main shock leave no doubt of an areal spread in the aftershock epicenters, but data are too limited to permit improvement of the spread previously given by Gutenberg (1943, p. 509) for 9 of the largest aftershocks. The circle in figure 3 is simply made large enough to include all of Gutenberg's epicenters.

Field reconnaissance in connection with this study points to the existence of a major northwest-trending active fault passing very nearly through the epicenter of the main shock (fig. 3). This fault is well delineated by the broad trough—of which Lower Covington Flat is a part—that extends some 12 miles southeast from Yucca Valley. The anomalous topography is especially well marked where this trough is crossed perpendicularly by the drainage of Smith Water Canyon. That this trough truly represents an active fault is indicated not only by its exceptional linearity throughout, but also, north of Covington Spring, by Recent scarplets and a broad zone of crushed rock. It seems probable that the Covington Flat earthquakes were caused by breaking along this fault, although the pattern of the aftershock epicenters is not sufficiently systematic to permit inference either of the trend of the break or of the dip of the fault plane.

Kitching Peak earthquakes.—The Kitching Peak earthquakes of 1944 and 1945 (table 5) occurred in the mountainous country between the Banning and Mission Creek faults about 25 km. west of Desert Hot Springs (fig. 3). This series, like the Morongo Valley shocks, had many of the characteristics of an earthquake "swarm"; the largest shock ($M = 5.3$) was preceded by 6 others, 3 of which were of magnitude 4.0 or greater. There were two "principal" shocks on June 12, 1944, both of which caused minor damage in near-by communities (Bodle, 1946, p. 17).

Epicenters of the Kitching Peak earthquakes were located by time differences with respect to shock no. 1, which is placed at 33° 59½′ N, 116° 46½′ W. The arrival times at Palomar were clearly about one second late for nearly all these shocks, a conclusion that is supported by locations of more recent earthquakes in this area using near-by stations that were not in existence at the time of the Kitching Peak shocks. Starting with shock no. 4, most of the remaining activity was centered about 8 km. east-southeast of the initial epicenters, and the line between these two locations may represent the extent of fracturing. In table 4 and figure 3 the initial epicenter is indicated by location "A" and the southeasterly epicenter by location "B." Although all shocks have been placed in one of these two categories, there was some spread in their locations, and all of these earthquakes seem to be related events. Of the total strain release, 79 per cent was associated with epicenter "B."

The trend of 105° between epicenters "A" and "B" parallels the regional structural alignment, and the location of the shocks north of the Banning fault suggests that this fault dips north. This conclusion is borne out by two independent lines of evidence: (1) The Banning fault in this area is known to be a north-dipping thrust fault at the surface (Allen, 1957, p. 340), and (2) Dehlinger (1952, p. 171) concluded from his study of the initial motions of transverse waves of some of these shocks that the movements had been primarily vertical (thrust) rather than horizontal (strike-slip).

San Gorgonio Mountain earthquakes.—This series of earthquakes commenced on October 24, 1935, with a shock of magnitude 5.1 that was followed by a normal sequence of aftershocks of decreasing magnitude. The entire series lasted only about two weeks. The main shock was felt widely throughout southern California and caused minor damage in near-by communities, particularly at the resorts along Mill Creek (Neumann, 1937, p. 36). Gutenberg (1943, p. 508) gives an epicenter for the main shock at 34° 06′ N, 116° 48′ W, and the data are so limited that little modification of this location is possible on the basis of more recent travel-time curves. These shocks are located on the east side of San Gorgonio Mountain somewhat north of the Mill Creek fault (fig. 3). Although their location north of a major fault is similar to that of other earthquakes in this study and possibly indicates a northerly dip of the fault plane, the geologic evidence is contradictory; the limited exposures of the fault plane show both north and south dips in this area (Allen, 1957, p. 343, pl. 1).

References

Allen, Clarence R.
1957. "San Andreas Fault Zone in San Gorgonio Pass, Southern California," *Bull. Geol. Soc. Am.*, 68: 315–350.

Benioff, Hugo
1951. "Earthquakes and Rock Creep, Part I: Creep Characteristics of Rocks and the Origin of Aftershocks," *Bull. Seism. Soc. Am.*, 41: 31–62.
1955*a*. "Seismic Evidence for Crustal Structure and Tectonic Activity," in Arie Poldervaart, ed., "Crust of the Earth," Geol. Soc. Am. *Spec. Paper* 62, pp. 61–73.
1955*b*. "Mechanism and Strain Characteristics of the White Wolf Fault as Indicated by the Aftershock Sequence," Calif. Div. Mines *Bull.* 171, pp. 199–202.

Benioff, Hugo, *et al.*
1954. "Progress Report, Seismological Laboratory, California Institute of Technology, 1953," *Trans. Am. Geophys. Union*, 35: 979–987.

Bodle, Ralph R.
1946. "United States Earthquakes, 1944," U.S.C.G.S. *Serial* 682.

Dehlinger, Peter
1952. "Shear-wave Vibrational Directions and Related Fault Movements in Southern California Earthquakes," *Bull. Seism. Soc. Am.*, 42: 155–173.

Dibblee, T. W., Jr.
1954. "Geology of the Imperial Valley Region, California," in R. H. Jahns, ed., "Geology of Southern California," Calif. Div. Mines *Bull.* 170: 21–52.

Fairbairn, H. W.
1949. *Structural Petrology of Deformed Rocks* (Cambridge: Addison-Wesley Press), 344 pages.

Gutenberg, B.
1943. "Earthquakes and Structure in Southern California," *Bull. Geol. Soc. Am.*, 54: 499–526.
1951. "Revised Travel Times in Southern California," *Bull. Seism. Soc. Am.*, 41: 143–163.

1955. "Epicenter and Origin Time of the Main Shock on July 21 and Travel Times of the Major Phases," in "Earthquakes in Kern County, California, during 1952," Calif. Div. Mines *Bull.* 171: 157–163.

1956. "Effects of Ground on Shaking in Earthquakes," *Trans. Am. Geophys. Union,* 37: 757–760.

Gutenberg, B., and C. F. Richter

1942. "Earthquake Magnitude, Intensity, Energy, and Acceleration," *Bull. Seism. Soc. Am.,* 32: 163–191.

1956. "Earthquake Magnitude, Intensity, Energy, and Acceleration (Second Paper)," *Bull. Seism. Soc. Am.,* 46: 105–145.

Jeffreys, H., and K. E. Bullen

1940. *Seismological Tables* (London: Brit. Assoc. Adv. Sci.), 48 pages.

Murphy, L. M., and F. P. Ulrich

1951. "United States Earthquakes, 1948," U.S.C.G.S. *Serial* 746.

Neumann, Frank

1937. "United States Earthquakes, 1935," U.S.C.G.S. *Serial* 600.

1942. "United States Earthquakes, 1940," U.S.C.G.S. *Serial* 647.

Richter, Charles F.

1951. "Instrumental Study of the Manix Earthquakes," *Bull. Seism. Soc. Am.,* 41: 347–388.

1955*a*. "Foreshocks and Aftershocks," in "Earthquakes in Kern County, California, during 1952," Calif. Div. Mines *Bull.* 171: 177–197.

1955*b*. "Unidirectional Progression of Faulting" (abstract), *Science,* 122: 880.

St. Amand, Pierre

1956. "Two Proposed Measures of Seismicity," *Bull. Seism. Soc. Am.,* 46: 41–45.

U. S. Coast and Geod. Survey

1949. Abstracts of earthquake reports for the Pacific Coast and western mountain region, October, November, December, 1948, U.S.C.G.S. *Publ.* MSA-60.

CALIFORNIA INSTITUTE OF TECHNOLOGY,
PASADENA, CALIFORNIA.
(Division of the Geological Sciences, contribution no. 851.)